PROCEEDINGS B

royalsocietypublishing.org/journal/rspb

Research

Cite this article: Allen BJ, Wignall PB, Hill DJ, Saupe EE, Dunhill AM. 2020 The latitudinal diversity gradient of tetrapods across the Permo-Triassic mass extinction and recovery interval. *Proc. R. Soc. B* **287**: 20201125. http://dx.doi.org/10.1098/rspb.2020.1125

Received: 15 May 2020
Accepted: 22 May 2020

Subject Category:
Palaeobiology

Subject Areas:
palaeontology, ecology

Keywords:
climate change, greenhouse, biodiversity, sampling bias, Tetrapoda, mass extinction

Author for correspondence:
Bethany J. Allen
e-mail: eebja@leeds.ac.uk

Electronic supplementary material is available online at https://doi.org/10.6084/m9.figshare.c.5004878.

THE ROYAL SOCIETY PUBLISHING

The latitudinal diversity gradient of tetrapods across the Permo-Triassic mass extinction and recovery interval

Bethany J. Allen[1], Paul B. Wignall[1], Daniel J. Hill[1], Erin E. Saupe[2] and Alexander M. Dunhill[1]

[1]School of Earth and Environment, University of Leeds, Leeds, UK
[2]Department of Earth Sciences, University of Oxford, Oxford, UK

BJA, 0000-0003-0282-6407; EES, 0000-0002-0370-9897; AMD, 0000-0002-8680-9163

The decline in species richness from the equator to the poles is referred to as the latitudinal diversity gradient (LDG). Higher equatorial diversity has been recognized for over 200 years, but the consistency of this pattern in deep time remains uncertain. Examination of spatial biodiversity patterns in the past across different global climate regimes and continental configurations can reveal how LDGs have varied over Earth history and potentially differentiate between suggested causal mechanisms. The Late Permian–Middle Triassic represents an ideal time interval for study, because it is characterized by large-scale volcanic episodes, extreme greenhouse temperatures and the most severe mass extinction event in Earth history. We examined terrestrial and marine tetrapod spatial biodiversity patterns using a database of global tetrapod occurrences. Terrestrial tetrapods exhibit a bimodal richness distribution throughout the Late Permian–Middle Triassic, with peaks in the northern low latitudes and southern mid-latitudes around 20–40° N and 60° S, respectively. Marine reptile fossils are known almost exclusively from the Northern Hemisphere in the Early and Middle Triassic, with highest diversity around 20° N. Reconstructed terrestrial LDGs contrast strongly with the generally unimodal gradients of today, potentially reflecting high global temperatures and prevailing Pangaean super-monsoonal climate system during the Permo-Triassic.

1. Background

The latitudinal diversity gradient (LDG) is one of the largest scale and longest known patterns in ecology (e.g. [1–7]). Modern biodiversity (i.e. richness) gradients are broadly defined as unimodal, with high biodiversity near the equator and low biodiversity at the poles [4,6]. The specifics of these gradients differ among taxonomic and ecological groups [2–4,6], and research over the last decade has revealed greater variation in modern LDGs than previously recognized. For example, benthic marine species richness appears to peak at 10–20° N, whereas pelagic species richness appears bimodal, with peaks at 10–40° on either side of the equator [8–11].

Study of the fossil record suggests the shape of LDGs has also changed through time [5,12]. Dinosaur diversity may have been greatest at temperate latitudes throughout the Mesozoic [13], North American mammal diversity may have been distributed evenly across latitudes for much of the Cenozoic [14,15] and peaks in marine animal diversity may have drifted from the Southern to Northern Hemisphere over the course of the Phanerozoic [16,17].

Numerous drivers of LDGs have been proposed (e.g. [2,3,18–22]). Interaction between key processes, the complexity of feedback cycles, and the covariance of many environmental variables with latitude complicate efforts to isolate causal mechanisms [2–4,6,23]. Climate and landmass distribution, however, have been put forward consistently as potential explanatory variables. Climate, particularly temperature and water availability, has long been considered a key control on spatial patterns of terrestrial biodiversity

[5,12,14,15,17,24–26] because the distributions of species are limited by climatic tolerance [22,24,27–30].

LDG studies in deep time have suggested palaeoclimate regime is a major control on the shape and slope of LDGs. Icehouse periods have been associated with a sharp, unimodal equatorial richness peak and greenhouse periods with a bimodal distribution, characterized by shallow peaks at mid-latitudes of both the Northern and Southern Hemispheres [5,17,31]. This contrast has been attributed to the strength of the pole-to-equator temperature gradient between the two climate regimes [5,13,17], but may also reflect spatio-temporal variations in precipitation [14,22,25]. The distribution of continental landmasses may also structure global patterns of biodiversity by controlling the spatial distribution of relevant habitats, particularly shallow continental shelf area in marine ecosystems [32–35]. Although studies of modern LDGs continue to provide insight into potential generative mechanisms (e.g. [36–39]), examination of LDGs during intervals when climate and landmass distribution were considerably different to today may provide new perspectives on global biodiversity patterns and their associated processes [5,13,31].

The Late Permian to Middle Triassic (approx. 260–239 Ma) represents a period in Earth history that contrasts considerably with the present day. Large-scale volcanism associated with the Siberian Traps drove extreme climate change, which was exacerbated by amalgamation of most landmasses into the supercontinent Pangaea [40–42]. This drove environmental perturbations that resulted in the most catastrophic mass extinction event of all time at the end of the Permian, around 252 Ma [43]. A prolonged interval of extremely high temperatures, which peaked in the Olenekian (late Early Triassic) [44], along with ocean anoxia and acidification have been identified as key extinction mechanisms [43,45], with persistence of these conditions extending well into the Middle Triassic, delaying full structural recovery of marine ecosystems for as long as 50 million years [46]. On land, high temperatures and seasonal precipitation in central Pangaea resulted in drought [40,47–49], while purported ozone depletion, brought about by halogen gas release from the Siberian Traps, resulted in high UV-B levels that caused plant sterilization and extinction (e.g. [50,51]). Early Triassic temperatures at low latitudes are considered to have been beyond the tolerable long-term threshold for both plants and animals, driving extinction and poleward migration [44,52]. The climate of the Middle Triassic has received less attention, but is thought to have been characterized by continued aridity in lower latitudes, with cyclical temperature fluctuations overprinting a general trend of steady cooling after the final eruptions of the Siberian Traps in the Olenekian [41,42].

Tetrapods were profoundly affected by the Permo-Triassic mass extinction (PTME). In the immediate aftermath, Early Triassic tetrapod communities were composed almost entirely of 'disaster fauna' such as *Lystrosaurus*, a herbivorous burrowing synapsid [47,53–55]. Following recovery from the PTME, archosauromorphs (Sauria), a group that appeared in the Middle Permian, became the dominant terrestrial animals [55]. The first marine reptile fossils are known from the Olenekian and were highly diverse by the Anisian, including basal sauropterygians and ichthyosaurs [56].

Two previous studies have offered perspectives on the distribution of tetrapods across the Permo-Triassic boundary. Sun *et al*. [44] used oxygen isotopes in conodont apatite to examine sea surface temperature (SST) change across the Late Permian and Early Triassic, recovering remarkably high SSTs throughout the interval but particularly during the Smithian–Spathian Thermal Maximum (approx. 248 Ma), when equatorial SSTs may have approached 40° C. Their qualitative analysis of tetrapod occurrences revealed an equatorial 'tetrapod gap' in the Early Triassic, hypothesized to have occurred due to the extreme warm temperatures that may have approached or exceeded the thermal tolerances of both terrestrial and marine vertebrates (around 42° C [57]). Bernardi *et al*. [52] also examined the distribution of individual tetrapod skeletal and footprint occurrences through the extinction and recovery interval, finding evidence for a poleward shift in tetrapod abundance in the Northern Hemisphere, but only in the Induan (earliest Triassic). This biogeographic pattern is congruent with a study of tetrapods immediately prior to the PTME, which found higher tetrapod diversity at temperate than equatorial latitudes during the Middle–Late Permian [58].

Here, we explore further the terrestrial and marine Permo-Triassic fossil tetrapod record by comparing species-level tetrapod biodiversity across latitudinal bins. We apply coverage-based interpolation and squares extrapolation to reconstruct LDGs from the Late Permian (before the PTME), Early Triassic (in the aftermath of the PTME) and Middle Triassic (during recovery). These LDGs are then assessed in light of the hypothesis that higher diversity will be found in the cooler refugia of the mid to high latitudes during extreme greenhouse conditions, such as during the Late Permian to Middle Triassic.

2. Methods

We conducted an in-depth literature review to maximize the completeness and robustness of our Late Permian to Late Triassic dataset for tetrapods. All tetrapod fossils from the Wuchiapingian (early Late Permian) through Carnian (early Late Triassic) were downloaded from the Paleobiology Database (PBDB). Genus names from this download were used to conduct a systematic literature search in Google Scholar, and any new taxa and occurrences were added to the Paleobiology Database. Once completed, the same criteria were used to download the enlarged dataset (in October 2018) [59]. We reviewed each 'collection', representing fossils from a particular locality and considered to be of a similar age, to increase temporal resolution. A literature search for formation names was conducted, with publications that listed the ages of specific beds or members further refining the geological date of collections, where possible [59]. We streamlined the mode of preservation and taxon habitat categories, reduced to either 'body' or 'trace', and 'marine' or 'terrestrial', respectively. Finally, the modern latitude and longitude of fossil localities were rotated to their palaeo-position at the time of deposition by filtering occurrences on a stage-by-stage basis then using the PALEOMAP Global Plate Model [60], implemented in G-Plates (version 2.1.0) [61]. The final dataset constituted 3563 unique tetrapod occurrences assigned to stage level, with our search efforts contributing 490 of these occurrences (13.8%).

All subsequent data manipulation and plotting was carried out in R [62] using the 'tidyverse' suite of packages [63]. The final dataset was filtered to include only records representing unique species, comprising those identified to species level and those identified to coarser taxonomic levels but representing a clade not already within their spatio-temporal bin. Since abundance data in the Paleobiology Database are relatively incomplete and inconsistently applied, the presence of a species within any given collection was treated as a single occurrence.

Fossil occurrences dated to a single geological stage were used to produce raw sampled-in-bin tetrapod richness curves.

To compare tetrapod richness patterns across space between the Late Permian, Early Triassic and Middle Triassic, stage-level occurrences were binned using 20° latitudinal bands, from 90° S to 90° N (the central bin includes the equator, from 10° N to 10° S). Terrestrial and marine body fossils were analysed separately, with 'marine tetrapods' referring to species whose morphology indicates life in marine habitats. This informal group is polyphyletic and includes basal ichthyosaurs, sauropterygians, tanystropheids and thalattosaurs.

When reconstructing historical spatial biodiversity patterns, allowances must be made for the spatio-temporal unevenness of the fossil record [5,56,64–70]. LDGs in deep time can be estimated if sampling rates in the clade of interest are relatively high, and consideration is given to partitioning variation in richness likely attributable to sampling biases versus that likely attributable to biological patterns [71]. Furthermore, subsampling and extrapolation methods can help alleviate issues of sampling heterogeneity. Coverage-based approaches are currently the most effective approach for mitigating the effects of fossil record bias in large-scale biodiversity analyses [72,73].

We applied two analytical approaches to account for spatio-temporal sampling biases in occurrence data: coverage-based interpolation [74,75] and squares [76]. Both were applied to collections within latitudinal bins for the Late Permian, Early Triassic and Middle Triassic time intervals (analyses were repeated for individual stages, electronic supplementary material, figure S2). Only body fossils were used for these analyses, due to the biological non-equivalence of trace fossil and body fossil species; one animal can produce multiple trace fossils, and traces are not easily allied to individual body fossil species.

Richness estimates were generated using coverage-based interpolation following the approach of Dunne *et al*. [77] using the R package iNEXT [75]. This approach conducts coverage-based rarefaction using the equations of Chao & Jost [74] (analogous to shareholder quorum subsampling [64,72]) and extrapolation based on the Chao1 estimator. Extrapolated estimates were discarded if more than three times the observed sample size, as this suggests a high species-to-occurrence count ratio that indicates the bin under consideration is likely to be undersampled [75]. Bins containing fewer than three species were incompatible with subsampling and therefore excluded from analyses (electronic supplementary material, table S1). Coverage-based rarefaction curves are also presented (electronic supplementary material, figure S3) to illustrate the relationship between coverage and coverage-standardized diversity estimates in each bin [72,77].

In addition to coverage-based interpolation, richness estimates were generated using the squares method [76]. Squares is an extrapolator based on the proportion of singletons in a given sample and is considered more robust to biases arising from small sample sizes and uneven abundance distributions than other interpolation methods [73,76]. Squares richness estimates were produced using the equation stated by Alroy [76].

Finally, we tested whether variation in sampling intensity among time bins influenced richness estimates, particularly given the expected reduction in Early Triassic tetrapod occurrences following the PTME. We subsampled to the same number of collections in each time interval (Late Permian, Early Triassic and Middle Triassic) using a bootstrap routine. For each time bin, we randomly sampled 250 collections for terrestrial tetrapods and 30 collections for marine tetrapods. Collections were allocated to their corresponding latitudinal bin and species richness was quantified across collections within each bin. This process was repeated 100 times. Diversity curves were produced using the mean species diversity in each latitude bin across the 100 replicates, allowing for comparison of LDGs among time bins given an artificially fixed sampling intensity.

3. Results

(a) Sampling

Raw richness, squares and interpolation estimates produced similar diversity-through-time curves (electronic supplementary material, figure S1). The number of collections with terrestrial tetrapod body fossils was relatively consistent through time (Late Permian, 291; Early Triassic, 307; Middle Triassic, 354), while the number of collections containing marine tetrapods increased from the Early to Middle Triassic (Early Triassic, 32; Middle Triassic, 207). Curves of raw species richness by latitude bin produced by bootstrapping to the same number of collections for each time interval were near-identical to those using the full datatset (electronic supplementary material, figure S4).

(b) Terrestrial distribution

Terrestrial tetrapod occurrences were broadly distributed but clustered throughout the studied interval (figure 1*a*). Both squares and interpolation analyses of terrestrial tetrapods by latitude (figure 1*c*) show a consistent bimodal richness distribution throughout the Late Permian to Middle Triassic, with a persistent dip in diversity in the low southern latitudes. In the Northern Hemisphere, diversity peaked at 40° N in the Late Permian. By the Early Triassic, the peak in species diversity had shifted to the 20° N bin (figure 1*b*), with stage-level analyses indicating this occurred in the Olenekian (electronic supplementary material, figure S2b). In the Middle Triassic, the Northern Hemisphere peak returned to 40° N. The gradient in the Southern Hemisphere remained relatively unchanged throughout the Late Permian to Middle Triassic, characterized by a consistent 60° S diversity peak.

(c) Marine distribution

Marine tetrapods were generally restricted to the Northern Hemisphere during the Early and Middle Triassic, despite having a relatively broad longitudinal distribution (figure 1*a*). Early Triassic marine tetrapods were most diverse in the 20° N bin, with the only other occurrences found in the 40° N bin (figure 1*d*). The 20° N peak in biodiversity persisted into the Middle Triassic, but with new occupation of the equatorial and 20° S bins. The stage-level analyses generally show comparable trends to those seen in the epoch-level time bins, but often with fewer bins occupied, producing patchier and less constrained gradients (electronic supplementary material, figure S2).

(d) Comparison with modern latitudinal diversity gradients

The Early Triassic terrestrial LDG produced by interpolation was compared to LDGs of modern birds, mammals and amphibians (figure 2; modern data derived from BiodiversityMapping.org, as used by Saupe *et al*. [22]). The modern curves have unimodal distributions that peak at low latitudes (maximum diversity at 9.5° S for birds and amphibians, 2.5° N for mammals), whereas the Early Triassic terrestrial curve peaks at higher latitudes, with a clear bimodal distribution (maximum diversity at 32.5° N and 62.5° S).

4. Discussion

In contrast with gradients for modern terrestrial tetrapods, the Permo-Triassic terrestrial tetrapod gradient was likely bimodal

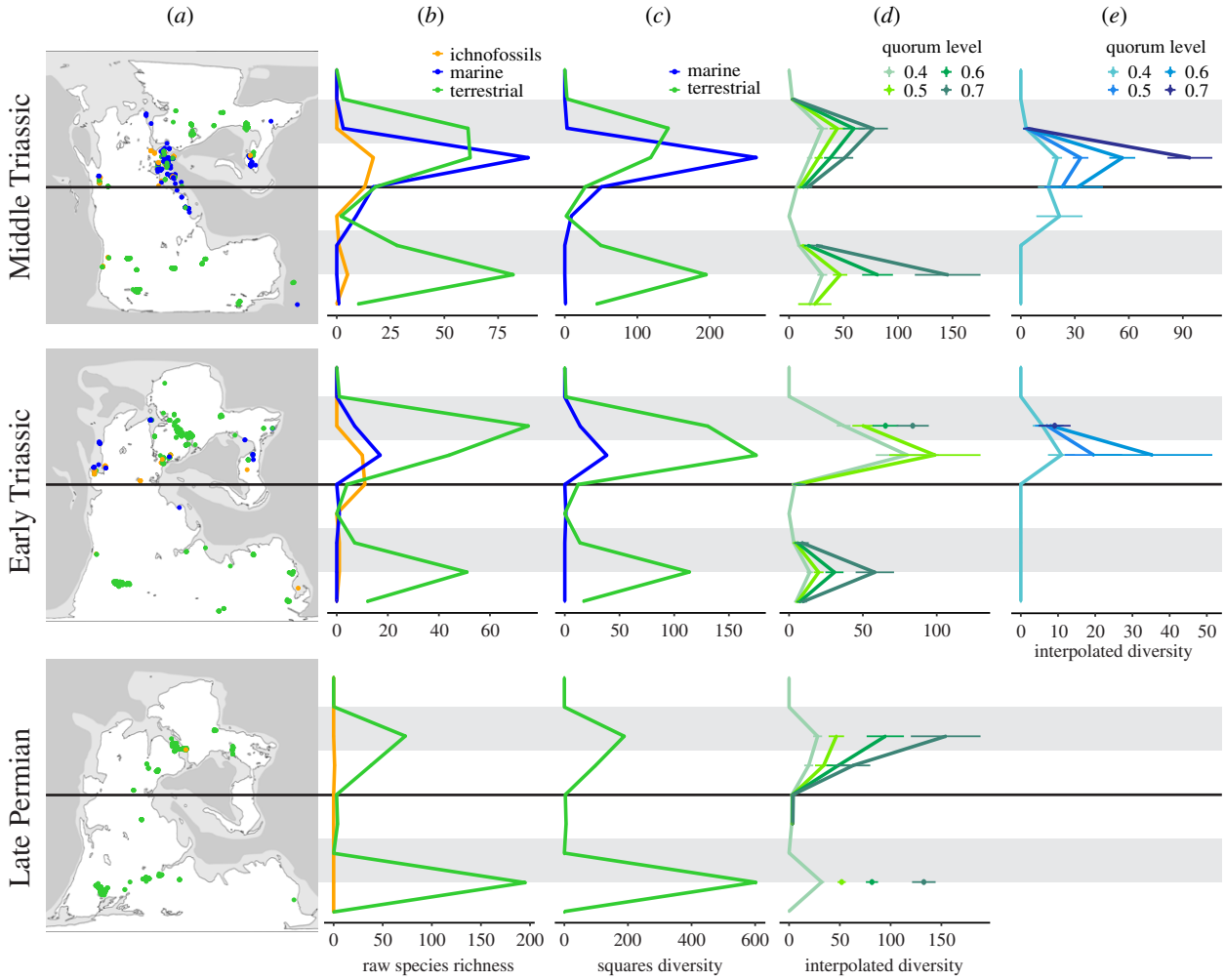

Figure 1. Tetrapod diversity by latitude in the Late Permian, Early Triassic and Middle Triassic. The grey bars indicate 30–60° N and S. (*a*) Palaeo-rotated occurrence locations plotted over maps from Scotese [59]; maps represent the Lopingian, Induan-Olenekian and Ladinian. (*b*) Raw occurrences within 20° latitude bins (e.g. central bin is 10° N–10° S). (*c*) Squares diversity by latitudinal bin for terrestrial (green) and marine (blue) tetrapods. (*d*,*e*) Interpolated diversity by latitudinal bin for terrestrial tetrapods (*d*) and marine tetrapods (*e*). Bins with less than three species have been plotted as '0', while missing points indicate an estimated diversity of more than three times the observed value. Error bars indicate 95% confidence intervals. The oldest marine tetrapod fossils are Olenekian (late Early Triassic; 251–247 Ma) in age.

with reduced diversity at low latitudes (10° N–30° S) (figure 1) [4,6]. The general shape of the terrestrial tetrapod richness gradient, particularly its bimodality, remained relatively constant throughout the Late Permian to Middle Triassic and may reflect the prevailing climate regime (greenhouse versus icehouse) [5,17,31]. Interestingly, the shape of the gradient did not seem affected by the PTME or even higher temperatures of the Early Triassic (equatorial SSTs increased from approx. 24° C in the latest Permian to approx. 40° C during the late Smithian [44]). Marine tetrapods, by contrast, maintained a diversity peak at low latitudes in the Northern Hemisphere from the Early to Middle Triassic (figure 1). The bimodal terrestrial LDG obtained here is comparable to the distribution of raw Early Triassic tetrapod occurrences from Sun *et al.* [44] and Bernardi *et al.* [52], and suggests continuity of LDG shape from the Middle Permian [58]. The shape of the gradient is also broadly comparable to the gradient of Mesozoic dinosaurs, which Mannion *et al.* [13] attributed to the distribution of land area during the break-up of Pangaea. This congruence suggests LDGs may have been bimodal for much of the Permian to mid Cenozoic, with modern LDGs only developing as global climate gradually cooled through the late Palaeogene and early Neogene [5,14,15,31].

Although latitude is a reasonable proxy for temperature in the modern, this relationship does not hold for the Triassic [41]. The latitudinal temperature gradient today largely reflects the operation of Hadley cells, but these cells may have collapsed in the Late Permian to give way to a more zonally asymmetric atmospheric system, with strong seasonal variation in temperature and precipitation [40,41,49]. Although the Tethyan coastal regions experienced supermonsoons, considerably less precipitation reached the continental interior, resulting in high aridity, particularly in the southern low to mid-latitudes [40,43]. Climate model reconstructions for the latest Permian suggest large areas of central Pangaea were desert, with seasonal average temperatures up to 45° C in the arid subtropics at 20–25° N and S [78]. Late Permian palaeoenvironmental evidence from localities in South Africa indicates considerable drought even at relatively high latitudes (approx. 65° S) [47]. Thus, much of the supercontinent interior may have been uninhabitable in the Late Permian, which could explain the bimodal, asymmetric tetrapod LDG reconstructed here. However, in contrast with Permian climates, Triassic climates have not been well studied [41,42], and the development of high-resolution climate models for the Triassic is essential for determining the

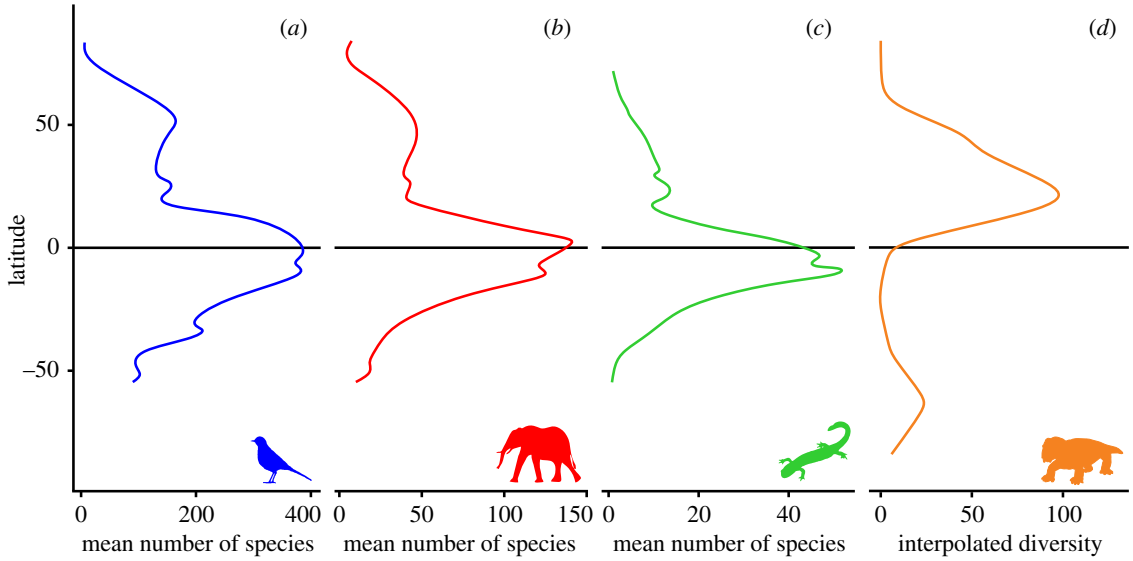

Figure 2. Smoothed latitudinal gradients for species of modern birds (*a*), mammals (*b*) and amphibians (*c*), compared with Early Triassic terrestrial tetrapods (as an example) based on interpolation analyses (*d*). Modern gradients derive from data obtained from BiodiversityMapping.org. Silhouettes are from Phylopic.org. (Online version in colour.)

key drivers of tetrapod extinction and migration during this interval.

We cautiously interpret the bimodal richness distributions found here as biologically meaningful, particularly given the agreement between the different sampling methodologies employed. In addition, collections from southern low latitude regions are consistently of low α-diversity (local diversity) throughout the entire Late Permian to Middle Triassic, in comparison with some very high levels of α-diversity in mid-latitude collections during the same intervals (electronic supplementary material, table S2). However, the spatial and temporal resolution of the analyses, and our certainty in the observed distributions representing biological patterns, would benefit from better geographic spread and higher density of samples [67–69]. New discoveries from the southern low to mid-latitudes could particularly help to distinguish between low biodiversity and poor sampling, but fossiliferous outcrops of this age and palaeolatitude are uncommon, particularly from terrestrial environments (electronic supplementary material, figure S5) [41,49,67]. Although extensive shallow and marginal marine deposits, such as those in Oman, are rich in invertebrate fossils (e.g. [79]), vertebrate fossils are known only from a handful of localities, such as Gour Laoud in Algeria (*Jesairosaurus lehmani*, *Odenwaldia* sp., indeterminate amphibians; palaeolatitude 9° S [80]) and Mariakani in Kenya (*Kenyasaurus mariakaniensis*; palaeolatitude 42° S [81]). Unfortunately, the age of fossils from these localities is poorly constrained and were therefore not included in our analyses.

Although broad stasis in bimodal richness gradients was observed over the approximately 23 million year interval considered here (Late Permian–Middle Triassic), smaller scale variability can be detected among time bins. Both squares and interpolation analyses suggest a shift in peak diversity in the Northern Hemisphere towards the equator in the Early Triassic, before returning to mid-latitudes in the Middle Triassic. This shift is also supported by the relatively high number of trace fossil occurrences in the equatorial and 20° N bins during the Early Triassic (figure 1*b*). An Early Triassic equatorward shift in diversity in the Northern Hemisphere seems surprising given that global temperatures were increasing at the time [44]. Instead, this shift may reflect differential sampling bias. Most of the interpolation rarefaction curves are exponential in shape, but the Early Triassic 20° N bin has a more asymptotic curve (electronic supplementary material, figure S3), indicating sampling completeness may be substantially higher in this bin relative to the others, inflating diversity estimates [72]. This peak in diversity corresponds to the high density of tetrapod fossils known from the Olenekian of Eastern Europe [82].

5. Conclusion

Our results suggest terrestrial tetrapods exhibited a bimodal richness distribution and were most diverse at mid-latitudes during the Late Permian–Middle Triassic. By contrast, marine tetrapods were generally restricted to northern low latitudes in the Early and Middle Triassic. Tetrapods were not excluded from equatorial regions during this interval, but were reduced in diversity at low southern latitudes. The bimodal LDG for terrestrial tetrapods during the Late Permian–Middle Triassic contrasts with the unimodal, equatorial diversity peaks exhibited by most terrestrial tetrapod clades in the modern, including birds, mammals and amphibians (figure 2). Permo-Triassic LDGs were likely shaped by the extreme climatic conditions of the time, particularly high global temperatures and heterogeneous precipitation. As is often the case regarding the vertebrate fossil record, our data are insufficient to determine conclusively whether observed patterns predominantly reflect true biological signal or heterogeneous spatial sampling. Further examination of Triassic climates and increased sampling intensity may advance our understanding of this time interval, providing greater insight into the potential influence of extreme greenhouse conditions on global patterns of biodiversity.

Ethics. No ethical considerations were required for this study.

Data accessibility. The datasets supporting this article have been uploaded as part of the electronic supplementary materials.

Authors' contributions. B.J.A. downloaded and reviewed the dataset, contributed additional Paleobiology Database entries, conducted statistical analyses and drafted the manuscript. All authors contributed to data interpretation and editing the manuscript. All authors also gave final approval for publication and agree to be held accountable for the work performed therein.

Competing interests. We have no competing interests to declare.

Funding. This work was supported by a Natural Environment Research Council studentship (NE/L002574/1) to B.J.A. This work was also supported by the Eco-PT grant (NE/P0137224/1), part of the Biosphere Evolutionary Transitions and Resilience (BETR) project, jointly funded by the Natural Environment Research Council, UK and National Natural Science Foundation, China (RG.EVEA.109961).

Acknowledgements. We thank members of the Palaeo@Leeds and Eco-PT research groups for discussion. We also thank Neil Brocklehurst, Matthew Powell and an anonymous reviewer, whose comments greatly improved this manuscript. B.J.A. is grateful to those who helped her with Paleobiology Database entry, particularly Graeme Lloyd and Richard Butler, and to Emma Dunne for discussion of methodology. Thanks to Yadong Sun for providing data for the conodont oxygen isotope curve. We also thank all who have contributed towards the Paleobiology Database collections used in this study. The Phylopic silhouettes used in figure 2 were contributed by an unknown artist, 'An Ignorant Atheist', 'zoosnow' and Steven Traver. This is Paleobiology Database publication no. 371.

References

1. von Humboldt A, Bonpland A. 2009 [1807] Essay on the geography of plants. In *Romanowski S, translator. Essay on the geography of plants* (ed. ST Jackson), pp. 49–144. Chicago, IL: University of Chicago Press.
2. Gaston KJ. 2000 Global patterns in biodiversity. *Nature* **405**, 220–227. (doi:10.1038/35012228)
3. Willig MR, Kaufman DM, Stevens RD. 2003 Latitudinal gradients of biodiversity: pattern, process, scale and synthesis. *Annu. Rev. Ecol. Evol. Syst.* **34**, 273–309. (doi:10.1146/annurev.ecolsys.34.012103.144032)
4. Hillebrand H. 2004 On the generality of the latitudinal diversity gradient. *Am. Nat.* **163**, 192–211. (doi:10.1086/381004)
5. Mannion PD, Upchurch P, Benson RBJ, Goswami A. 2014 The latitudinal diversity gradient through deep time. *TREE* **29**, 42–50. (doi:10.1016/j.tree.2013.09.012)
6. Kinlock NL *et al.* 2018 Explaining global variation in the latitudinal diversity gradient: meta-analysis confirms known patterns and uncovers new ones. *Global Eco. Biogeog.* **27**, 125–141. (doi:101111/geb.12665)
7. Saupe EE, Farnsworth A, Lunt DJ, Sagoo N, Pham KV, Field DJ. 2019*a* Climatic shifts drove major contractions in avian latitudinal distributions throughout the Cenozoic. *PNAS* **116**, 12 895–12 900. (doi:10.1073/pnas.1903866116)
8. Tittensor DP, Mora C, Jetz W, Lotze HK, Ricard D, Vanden Berghe E, Worm B. 2010 Global patterns and predictors of marine biodiversity across taxa. *Nature* **466**, 1098–1101. (doi:10.1038/nature09329)
9. Powell MG, Beresford VP, Colaianne BA. 2012 The latitudinal position of peak marine diversity in living and fossil biotas. *J. Biogeogr.* **39**, 1687–1694. (doi:10.1111/j.1365-2699.2012.02719.x)
10. Chaudhary C, Saeedi H, Costello MJ. 2016 Bimodality of latitudinal diversity gradients in marine species richness. *TREE* **31**, 670–676. (doi:10.1016/j.tree.2016.06.001)
11. Chaudhary C, Saeedi H, Costello MJ. 2017 Marine species richness is bimodal with latitude: a reply to Fernandez and Marques. *TREE* **32**, 234–237. (doi:10.1016/j.tree.2017.02.007)
12. Crame JA. 2001 Taxonomic diversity gradients through geological time. *Divers. Distrib.* **7**, 175–189. (doi:10.1111/j.1472-4642.2001.00106.x)
13. Mannion PD, Benson RBJ, Upchurch P, Butler RJ, Carrano MT, Barrett PM. 2012 A temperate palaeodiversity peak in Mesozoic dinosaurs and evidence for Late Cretaceous geographical partitioning. *Global Eco. Biogeog.* **21**, 898–908. (doi:10.1111/j.1466-8238.2011.00735.x)
14. Fraser D, Hassall C, Gorelick R, Rybczynski N. 2014 Mean annual precipitation explains spatiotemporal patterns of Cenozoic mammal beta diversity and latitudinal diversity gradients in North America. *PLoS ONE* **9**, e106499. (doi:10.1371/journal.pone.0106499)
15. Marcot JD, Fox DL, Niebuhr SR. 2016 Late Cenozoic onset of the latitudinal diversity gradient of North American mammals. *PNAS* **113**, 7189–7194. (doi:10.1073/pnas.1524750113)
16. Powell MG. 2009 The latitudinal diversity gradient of brachiopods over the past 530 million years. *J. Geol.* **117**, 585–594. (doi:10.1086/605777)
17. Naimark EB, Markov AV. 2011 Northward shift in faunal diversity: a general pattern of evolution of Phanerozoic marine biota. *Biol. Bull. Rev.* **1**, 71–81.
18. Clarke A, Gaston KJ. 2006 Climate, energy and diversity. *Proc. R. Soc. B* **273**, 2257–2266. (doi:10.1098/rspb.2006.3545)
19. Mittelbach GG *et al.* 2007 Evolution and the latitudinal diversity gradient: speciation, extinction and biogeography. *Ecol. Lett.* **10**, 315–331. (doi:10.1111/j.1461-0248.2007.01020.x)
20. Schemske DW, Mittelbach GG, Cornell HV, Sobel JM, Roy K. 2009 Is there a latitudinal diversity gradient in the importance of biotic interactions? *Annu. Rev. Ecol. Evol. Syst.* **40**, 245–269. (doi:10.1146/annurev.ecolsys.39.110707.173430)
21. Archibald SB, Bossert WH, Greenwood DR, Farrell BD. 2010 Seasonality, the latitudinal gradient of diversity, and Eocene insects. *Paleobiology* **36**, 374–398. (doi:10.1666/09021.1)
22. Saupe EE, Myers CE, Peterson AT, Soberón J, Singarayer J, Valdes P, Qiao H. 2019 Spatio-temporal climate change contributes to latitudinal diversity gradients. *Nature Ecol. Evol.* **3**, 1419–1429. (doi:10.1038/s41559-019-0962-7)
23. Jablonski D. 2008 Extinction and the spatial dynamics of biodiversity. *PNAS* **105**, 11 528–11 535. (doi:10.1073/pnas.0801919105)
24. Brown JH. 1984 On the relationship between abundance and distribution of species. *Am. Nat.* **124**, 255–279. (doi:10.1086/284267)
25. Hawkins BA *et al.* 2003 Energy, water, and broad-scale geographic patterns of species richness. *Ecology* **84**, 3105–3117. (doi:10.1890/03-8006)
26. Currie DJ *et al.* 2004 Predictions and tests of climate-based hypotheses of broad-scale variation in taxonomic richness. *Ecol. Lett.* **7**, 1121–1134. (doi:10.1111/j.1461-0248.2004.00671.x)
27. Grinnell J. 1917 The niche-relationships of the California Thrasher. *The Auk* **34**, 427–433. (doi:10.2307/4072271)
28. Hutchinson GE. 1957 Concluding remarks. *Cold Spring Harbour Symp. Quant. Biol.* **22**, 415–427.
29. Root T. 1988 Energy constraints on avian distributions and abundances. *Ecology* **69**, 330–339.
30. Powell MG. 2007 Geographic range and genus longevity of late Paleozoic brachiopods. *Paleobiology* **33**, 530–546. (doi:10.1666/07011.1)
31. Meseguer AS, Condamine FL. 2020 Ancient tropical extinctions at high latitudes contributed to the latitudinal diversity gradient. *Evolution*. (doi:10.1111/evo.13967)
32. Valentine JW, Moores EM. 1970 Plate-tectonic regulation of faunal diversity and sea level: a model. *Nature* **228**, 657–659.
33. Mannion PD, Benson RBJ, Carrano MT, Tennant JP, Judd J, Butler RJ. 2015 Climate constrains the evolutionary history and biodiversity of crocodylians. *Nat. Commun.* **6**, 8438. (doi:10.1038/ncomms9438)
34. Vavrek MJ. 2016 The fragmentation of Pangaea and Mesozoic terrestrial vertebrate biodiversity. *Biol. Lett.* **12**, 20160528. (doi:10.1098/rsbl.2016.0528)
35. Zaffos A, Finnegan S, Peters SE. 2017 Plate tectonic regulation of global marine animal diversity. *PNAS* **114**, 5653–5658. (doi:10.1073/pnas.1702297114)
36. Buckley LB *et al.* 2010 Phylogeny, niche conservatism and the latitudinal diversity gradient in mammals. *Proc. R. Soc. B* **277**, 2131–2138. (doi:10.1098/rspb.2010.0179)
37. Condamine FL, Sperling FAH, Wahlberg N, Rasplus J-Y, Kergoat GJ. 2012 What causes latitudinal gradients in species diversity? Evolutionary processes and ecological constraints on swallowtail biodiversity. *Ecol. Lett.* **15**, 267–277. (doi:10.1111/j.1461-0248.2011.01737.x)
38. Jetz W, Fine PVA. 2012 Global gradients in vertebrate diversity predicted by historical area-productivity dynamics and contemporary environment. *PLoS Biol.* **10**, e1001292. (doi:10.1371/journal.pbio.1001292)
39. Pyron RA, Wiens JJ. 2013 Large-scale phylogenetic analyses reveal the causes of high tropical amphibian diversity. *Proc. R. Soc. B* **280**, 20131622. (doi:10.1098/rspb.2013.1622)
40. Parrish JT. 1993 Climate of the supercontinent Pangea. *J. Geol.* **101**, 215–233. (doi:10.1086/648217)

41. Preto N, Kustatscher E, Wignall PB. 2010 Triassic climates — state of the art and perspectives. *Palaeo3* **290**, 1–10. (doi:10.1016/j.palaeo.2010.03.015)
42. Trotter JA, Williams IS, Nicora A, Mazza M, Rigo M. 2015 Long-term cycles of Triassic climate change: a new $\delta^{18}O$ record from conodont apatite. *Earth Plan. Sci. Lett.* **415**, 165–174. (doi:10.1016/j.epsl.2015.01.038)
43. Wignall PB. 2015 *The worst of times: how life on earth survived eighty million years of extinctions*, 199 p. Princeton, NJ: Princeton University Press.
44. Sun Y, Joachimski MM, Wignall PB, Yan C, Chen Y, Jiang H, Wang L, Lai X. 2012 Lethally hot temperatures during the Early Triassic greenhouse. *Science* **338**, 366–370. (doi:10.1126/science.1224126)
45. Penn JL, Deutsch C, Payne JL, Sperling EA. 2018 Temperature-dependent hypoxia explains biogeography and severity of end-Permian marine mass extinction. *Science* **362**, eaat1327. (doi:10.1126/science.aat1327)
46. Song H, Wignall PB, Dunhill AM. 2018 Decoupled taxonomic and ecological recoveries from the Permo-Triassic extinction. *Sci. Adv.* **4**, eaat5091. (doi:10.1126/sciadv.aat5091)
47. Smith RMH, Botha-Brink J. 2014 Anatomy of a mass extinction: sedimentological and taphonomic evidence for drought-induced die-offs at the Permo-Triassic boundary in the main Karoo Basin, South Africa. *Palaeo3* **396**, 99–118. (doi:10.1016/j.palaeo.2014.01.002)
48. Looy CV *et al.* 2016 Biological and physical evidence for extreme seasonality in central Permian Pangea. *Palaeo3* **451**, 210–226. (doi:10.1016/j.palaeo.2016.02.016)
49. Tabor NJ, Sidor CA, Smith RMH, Nesbitt SJ, Angielczyk KD. 2018 Paleosols of the Permian-Triassic: proxies for rainfall, climate change, and major changes in terrestrial tetrapod diversity. *J. Vert. Paleo.* **37**, S240–S253. (doi:10.1080/02724634.2017.1415211)
50. Beerling DJ, Harfoot M, Lomax B, Pyle JA. 2007 The stability of the stratospheric ozone layer during the end-Permian eruption of the Siberian Traps. *Phil. Trans. R. Soc. A* **365**, 1843–1866. (doi:10.1098/rsta.2007.2046)
51. Benca JP, Duijnstee IAP, Looy CV. 2018 UV-B–induced forest sterility: implications of ozone shield failure in Earth's largest extinction. *Sci. Adv.* **4**, e1700618. (doi:10.1126/sciadv.1700618)
52. Bernardi M, Petti FM, Benton MJ. 2018 Tetrapod distribution and temperature rise during the Permian–Triassic mass extinction. *Proc. R. Soc. B* **285**, 20172331. (doi:10.1098/rspb.2017.2331)
53. Sidor CA, Vilhena DA, Angielczyk KD, Huttenlocker AK, Nesbitt SJ, Peecook BR, Steyer JS, Smith RMH, Tsuji LA. 2013 Provincialization of terrestrial faunas following the end-Permian mass extinction. *PNAS* **110**, 8129–8133. (doi:10.1073/pnas.1302323110)
54. Button DJ, Lloyd GT, Ezcurra MD, Butler RJ. 2017 Mass extinctions drove increased global faunal cosmopolitanism on the supercontinent Pangaea. *Nat. Commun.* **8**, 733. (doi:10.1038/s41467-01700827-7)
55. Ezcurra MD, Butler RJ. 2018 The rise of the ruling reptiles and ecosystem recovery from the Permo-Triassic mass extinction. *Proc. R. Soc. B* **285**, 20180361. (doi:10.1098/rspb.2018.0361)
56. Benson RBJ, Butler RJ. 2011 Uncovering the diversification history of marine tetrapods: ecology influences the effect of geological sampling biases. *Geol. Soc. Lond., Spec. Pub.* **358**, 191–208. (doi:10.1144/SP358.13)
57. Pörtner HO. 2002 Climate variations and the physiological basis of temperature dependent biogeography: systemic to molecular hierarchy of thermal tolerance in animals. *Comp. Biochem. Physiol. A* **132**, 739–761. (doi:10.1016/S1095-6433(02)00045-4)
58. Brocklehurst N, Day MO, Rubidge BS, Fröbisch J. 2017 Olson's Extinction and the latitudinal biodiversity gradient of tetrapods in the Permian. *Proc. R. Soc. B* **284**, 20170231. (doi:10.1098/rspb.2017.0231)
59. Allen BJ, Wignall PB, Hill DJ, Saupe EE, Dunhill AM. 2020 Data from: The latitudinal diversity gradient of tetrapods across the Permo-Triassic mass extinction and recovery interval. Dryad Digital Repository. (doi:10.5061/dryad.m63xsj3zk)
60. Scotese CR. 2016 PALEOMAP PaleoAtlas for GPlates and the PaleoData Plotter Program. Version 2. PALEOMAP Project. See http://www.earthbyte.org/paleomap-paleoatlas-for-gplates/.
61. Müller RD *et al.* 2018 GPlates: building a virtual Earth through deep time. *Geochem. Geophys. Geosyst.* **19**, 2243–2261. (doi:10.1029/2018GC007584)
62. R Core Team. 2018 *R: a language and environment for statistical computing*. Version 3.5.1. Vienna, Austria: R Foundation for Statistical Computing. See https://www.r-project.org/.
63. Wickham H. 2017 tidyverse: Easily install and load the 'tidyverse'. Version 1.2.1. See https://cran.r-project.org/package=tidyverse.
64. Alroy J. 2010 Geographical, environmental and intrinsic biotic controls on Phanerozoic marine diversification. *Palaeontology* **53**, 1211–1235. (doi:10.1111/j.1475-4983.2010.01011.x)
65. Benson RBJ, Butler RJ, Lindgren J, Smith AS. 2010 Mesozoic marine tetrapod diversity: mass extinctions and temporal heterogeneity in geological megabiases affecting vertebrates. *Proc. R. Soc. B* **277**, 829–834. (doi:10.1098/rspb.2009.1845)
66. Benton MJ, Dunhill AM, Lloyd GT, Marx FG. 2011 Assessing the quality of the fossil record: insights from vertebrates. *Geol. Soc. Lond., Spec. Pub.* **358**, 63–94. (doi:10.1144/SP358.6)
67. Benson RBJ, Upchurch P. 2013 Diversity trends in the establishment of terrestrial vertebrate ecosystems: interactions between spatial and temporal sampling biases. *Geology* **41**, 43–46. (doi:10.1130/G33543.1)
68. Vilhena DA, Smith AB. 2013 Spatial bias in the marine fossil record. *PLoS ONE* **8**, e74470. (doi:10.1371/journal.pone.0074470)
69. Close RA, Benson RBJ, Upchurch P, Butler RJ. 2017 Controlling for the species-area effect supports constrained long-term Mesozoic terrestrial vertebrate diversification. *Nat. Commun.* **8**, 15381. (doi:10.1038/ncomms15381)
70. Darroch SA, Saupe EE. 2018 Reconstructing geographic range-size dynamics from fossil data. *Paleobiology* **44**, 25–39. (doi:10.1017/pab.2017.25)
71. Fraser D. 2017 Can latitudinal richness gradients be measured in the terrestrial fossil record? *Paleobiology* **43**, 479–494. (doi:10.1017/pab.2017.2)
72. Close RA, Evers SW, Alroy J, Butler RJ. 2018 How should we estimate diversity in the fossil record? Testing richness estimators using sampling-standardised discovery curves. *Meth. Ecol. Evol.* **9**, 1386–1400. (doi:10.1111/2041-210x.12987)
73. Alroy J. 2020 On four measures of taxonomic richness. *Paleobiology* 1–18. (doi:10.1017/pab.2019.40)
74. Chao A, Jost L. 2012 Coverage-based rarefaction and extrapolation: standardizing samples by completeness rather than size. *Ecology* **93**, 2533–2547. (doi:10.1890/11-1952.1)
75. Hsieh TC, Ma KH, Chao A. 2016 iNEXT: an R package for rarefaction and extrapolation of species diversity (Hill numbers). *Meth. Ecol. Evol.* **7**, 1451–1456. (doi:10.1111/2041-210X.12613)
76. Alroy J. 2018 Limits to species richness in terrestrial communities. *Ecol. Lett.* **21**, 1781–1789. (doi:10.1111/ele.13152)
77. Dunne EM, Close RA, Button DJ, Brocklehurst N, Cashmore DD, Lloyd GT, Butler RJ. 2018 Diversity change during the rise of tetrapods and the impact of the 'Carboniferous rainforest collapse'. *Proc. R. Soc. B* **285**, 20172730. (doi:10.1098/rspb.2017.2730)
78. Roscher M, Stordal F, Svensen H. 2011 The effect of global warming and global cooling on the distribution of the latest Permian climate zones. *Palaeo3* **309**, 186–200. (doi:10.1016/j.palaeo.2011.05.042)
79. Krystyn L, Richoz S, Baud A, Twitchett RJ. 2003 A unique Permian-Triassic boundary section from the Neotethyan Hawasina Basin, Central Oman Mountains. *Palaeo3* **191**, 329–344. (doi:10.1016/S0031-0182(02)00670-3)
80. Jalil N-E. 1999 Continental Permian and Triassic vertebrate localities from Algeria and Morocco and their stratigraphical correlations. *J. African Ear. Sci.* **29**, 219–226. (doi:10.1016/S0899-5362(99)00091-3)
81. Harris JM, Carroll RL. 1977 *Kenyasaurus*, a new eosuchian reptile from the Early Triassic of Kenya. *J. Palaeo.* **51**, 139–149.
82. Shishkin MA, Novikov IV. 2017 Early stages of recovery of the East European tetrapod fauna after the end-Permian crisis. *Paleo. J.* **51**, 612–622. (doi:10.1134/S0031030117060089)